

Supplementary Information for

Borohydrides: From Sheet to Framework Topologies

P. Schouwink, M. B. Ley, T. R. Jensen, L. Smrčok, and R. Černý

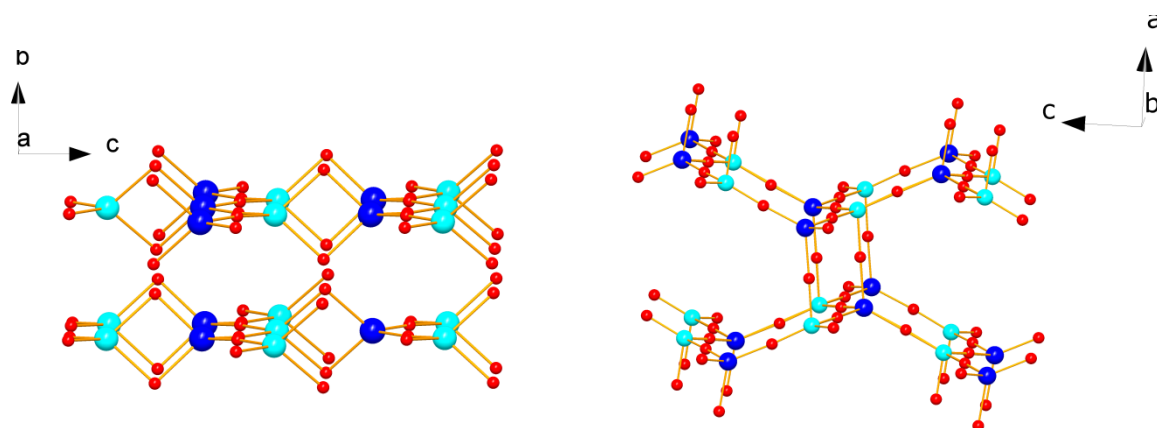


Figure S1 Left, two isolated sheets of $\text{KLiMg}(\text{BH}_4)_4$, out of plane B atoms are bridging ligands of shared edges. Right, fragment of the 3D framework in a hypothetical compound $\text{LiMg}(\text{BH}_4)_4^-$. Buckled sheets are interconnected in a – direction by B, that in the case of $\text{KLiMg}(\text{BH}_4)_4$ pertain to shared edges. Both models are viewed along the sheets.

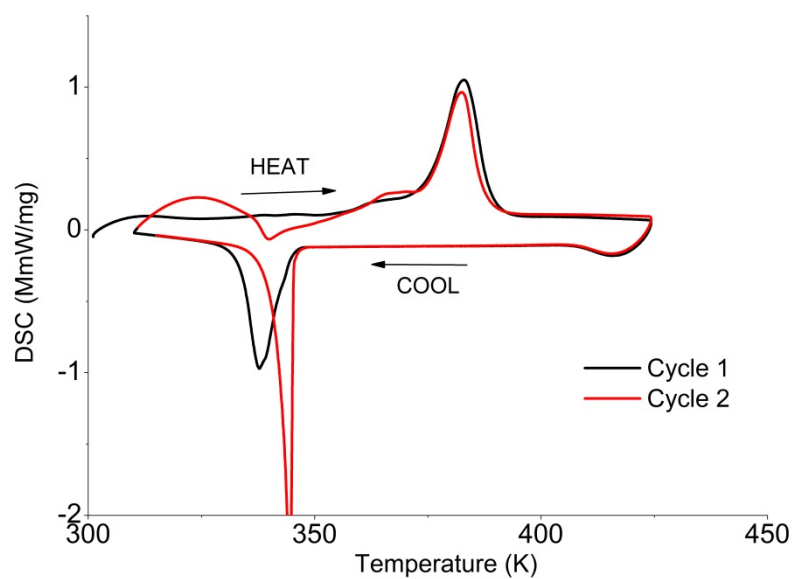


Figure S2. Differential scanning calorimetry shown for the sample $1\text{KBH}_4 + 1\text{LiBH}_4 + 1\text{Mg}(\text{BH}_4)_2$, run in 2 cycles.

Model	a [Å]	b [Å]	c [Å]	α [°]	β [°]	γ [°]	V [Å ³]
1	8.0057	9.5476	12.616	90.0005	89.9998	88.9421	964.14
2	7.9542	9.5085	12.85	90.0001	90.0069	89.9995	971.88
3	7.8865	9.6436	12.804	90.0055	90.0001	90.0000	973.80
4	7.9629	9.5477	12.7234	90.0127	89.9009	88.9982	967.18
5	7.9966	9.4231	12.6554	89.9993	90.0003	90.0015	953.62
6	7.965	9.5366	12.7266	89.9922	90.1362	90.9389	966.70
Dimeric	7.9932	9.4142	12.7314	89.6141	89.7975	88.0378	957.44

Table S1: Lattice parameters of optimized models presented in table S1 (above).

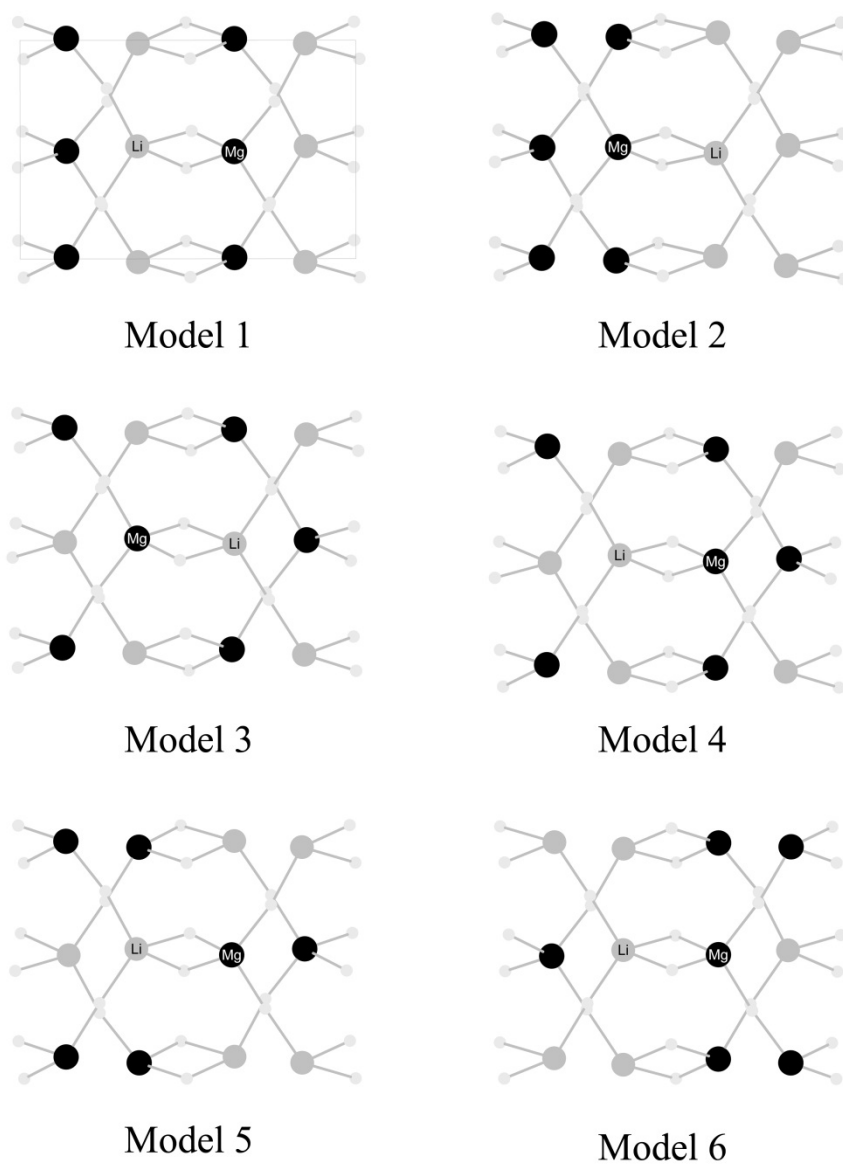


Figure S3. Schematic view along the b -axis of ordered models optimized by DFT, for the returned energies see table S1, above. Li atoms are in dark grey, Mg atoms in black. B-linkers are shown in light grey to visualize the pseudo-hexagonal arrangement in sheets.

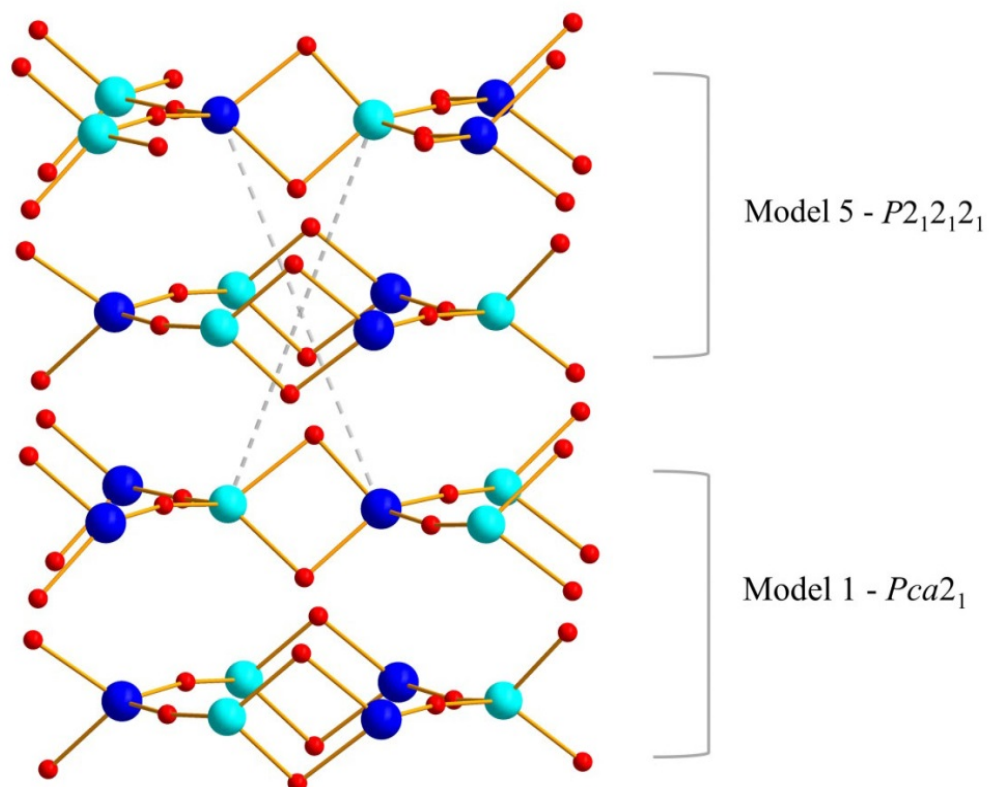


Figure S4. Alternate stacking of Model 1 and Model 5, producing an inversion center across the interface relating Li and Mg atoms of every second sheet, as visualized by the broken lines.

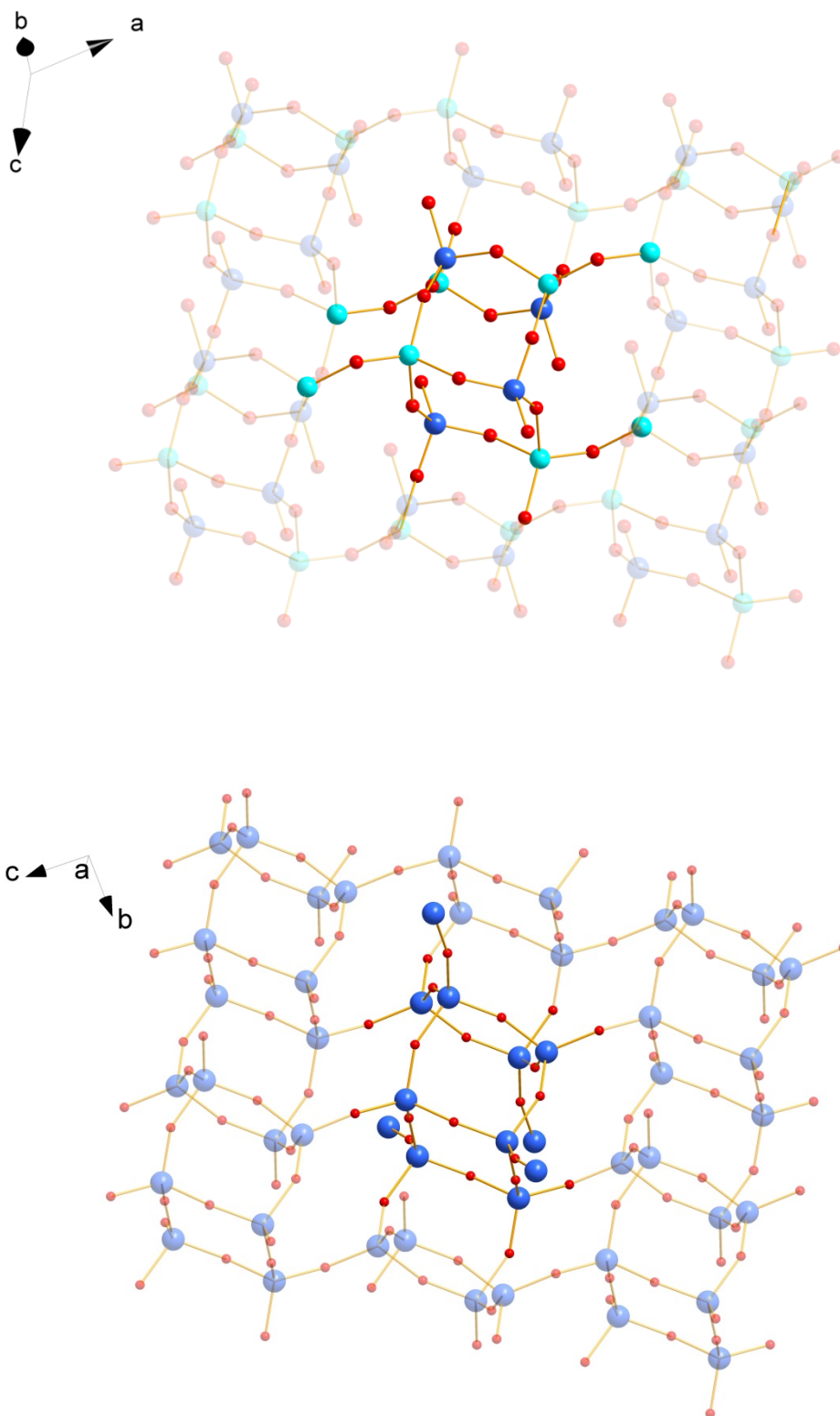


Figure S5. Double layered sheet in $K_3Li_2Mg_2(BH_4)_9$ (top) and $\beta-Mg(BH_4)_2$ (bottom). The connectivity between four-fold rings within and between layers is emphasized, showing terminal B atoms coordinating to Mg centers and bridging B atoms coordinating to Li that interconnect rings within the same layer. In $\beta-Mg(BH_4)_2$ (bottom), the BH_4 -groups that are terminal in the case of $K_3Li_2Mg_2(BH_4)_9$, bridge to the neighbouring sheets, the Mg-atoms belonging to the latter are also drawn in bold.

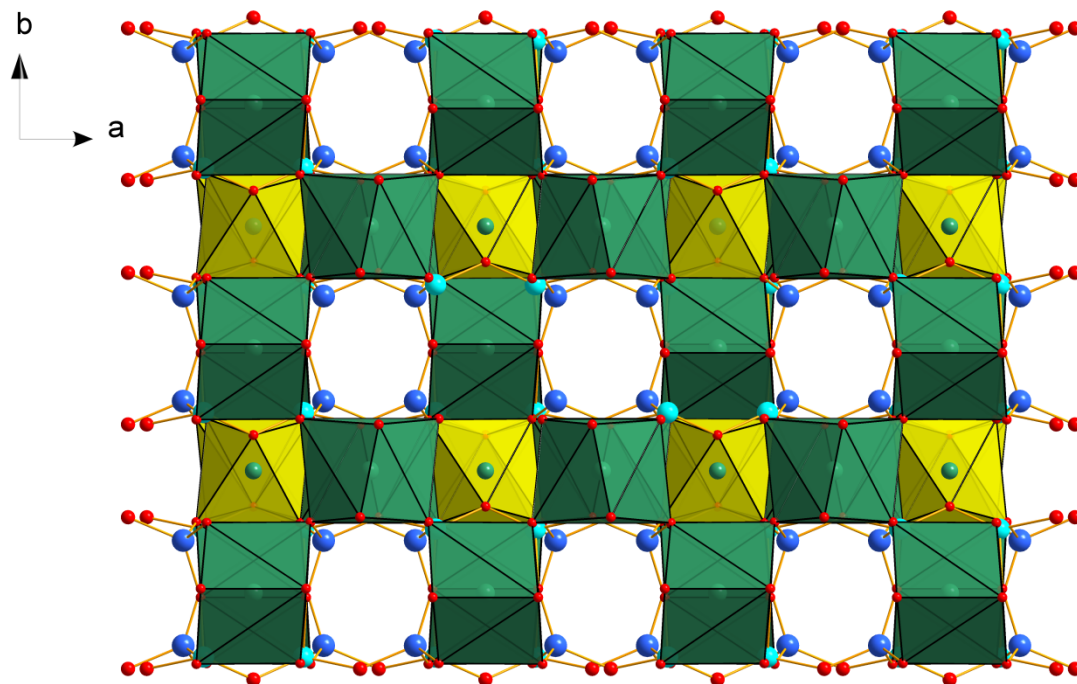


Figure S6. A view of $K_3Li_2Mg_2(BH_4)_9$ along the c-axis, showing coordination polyhedra of potassium positions. The view is along the double-layered sheets, that lie in the (ac) -plane.

Table S2 Atomic coordinates of $\text{KLiMg}(\text{BH}_4)_4$, space group $Aba2$, $a = 8.166(2)$, $b = 9.168(3)$, $c = 12.539(1)$ Å, $V = 939(2)$ Å³, $Z = 4$ at RT as refined from synchrotron powder diffraction data measured at SNBL. Standard deviations for hydrogen atoms positions were retrieved by the boot strapping method implemented in TOPAS.

Atom	Site	x	y	z	Occupancy	B_{iso} [Å ²]
K		0	0	0.692(5)	1	4.5(2)
Mg1		0	0	0.0538(4)	0.15(1)	3.7(2)
Li1		0	0	0.0538(4)	0.85(1)	3.7(2)
Li2		0	0	0.336(9)	0.15(1)	3.7(2)
Mg2		0	0	0.336(9)	0.85(1)	3.7(2)
B1		0.738(2)	0.509(1)	0.444(1)	1	2.0(3)
H11		0.674(8)	0.595(5)	0.395(4)	1	B_{B1}
H12		0.844(6)	0.463(7)	0.397(4)	1	B_{B1}
H13		0.649(7)	0.419(5)	0.464(5)	1	B_{B1}
H14		0.786(8)	0.559(6)	0.521(3)	1	B_{B1}
B2		0.6032(7)	0.823(8)	0.697(2)	1	B_{B1}
H21		0.533(7)	0.782(7)	0.626(4)	1	B_{B1}
H22		0.649(7)	0.938(3)	0.681(6)	1	B_{B1}
H23		0.711(5)	0.749(5)	0.713(6)	1	B_{B1}
H24		0.520(7)	0.824(9)	0.769(4)	1	B_{B1}

Table S3 Selected interatomic distances in $\text{KLiMg}(\text{BH}_4)_4$, for the structure refined at room temperature.

K-K	6.14(1)-7.77(2) Å
LiMg1-LiMg1	6.14(2)-7.77(2) Å
LiMg2-LiMg2	6.14(2)-7.77(2) Å
K-B	3.09(1)-3.81(1) Å
LiMg1-B	2.54(2)-2.56(3) Å
LiMg2-B	2.37(1)-2.52(2) Å
B-H	1.13(2) Å

Table S4 Atomic coordinates of $\text{KLiMn}(\text{BH}_4)_4$, space group $Aba2$, $a = 8.204(2)$, $b = 9.168(3)$, $c = 12.592(3)$ Å, $V = 951(1)$ Å³, $Z = 4$ at RT as refined from synchrotron powder diffraction data measured at SNBL. Standard deviations for hydrogen atoms positions were retrieved by the boot strapping method implemented in TOPAS.

Atom	Site	x	y	z	Occupancy	B_{iso} [Å ²]
K		0	0	0.720(3)	1	3.5(3)
Mn1		0	0	0.071(4)	0.85(1)	2.4(1)
Li1		0	0	0.071(4)	0.15(1)	2.4(1)
Li2		0	0	0.340(3)	0.85(1)	2.4(1)
Mn2		0	0	0.340(3)	0.15(1)	2.4(1)
B1		0.727(8)	0.507(7)	0.469(8)	1	1.8(4)
H11		0.67(1)	0.56(2)	0.42(5)	1	B_{B1}
H12		0.83(3)	0.46(4)	0.42(4)	1	B_{B1}
H13		0.64(1)	0.42(2)	0.48(2)	1	B_{B1}
H14		0.78(4)	0.55(2)	0.55(2)	1	B_{B1}
B2		0.689(9)	0.814(7)	0.707(4)	1	B_{B1}
H21		0.54(4)	0.77(2)	0.64(2)	1	B_{B1}
H22		0.65(1)	0.93(2)	0.69(4)	1	B_{B1}
H23		0.72(2)	0.74(4)	0.72(4)	1	B_{B1}
H24		0.53(4)	0.81(4)	0.78(5)	1	B_{B1}

Table S5 Selected interatomic distances in $\text{KLiMn}(\text{BH}_4)_4$, for the structure refined at room temperature.

K-K	6.15(3)-7.79(2) Å
LiMn1-LiMn1	6.15(3)-7.79(2) Å
LiMn2-LiMn2	6.15(3)-7.79(2) Å
K-B	3.03(1)-3.84(1) Å
LiMn1-B	2.58(3) Å
LiMn2-B	2.48(1)-2.55(2) Å
B-H	1.13(2) Å

Table S6 Atomic coordinates of RbLiMg(BH₄)₄, space group *Aba2*, $a = 8.234(1)$, $b = 9.485(2)$, $c = 12.577(2)$ Å, $V = 982(1)$ Å³, $Z = 4$ at *RT* as refined from synchrotron powder diffraction data measured at SLS. Standard deviations for hydrogen atoms positions were retrieved by the boot strapping method implemented in TOPAS.

Atom	Site	<i>x</i>	<i>y</i>	<i>z</i>	Occupancy	B_{iso} [Å ²]
Rb1		0	0	0.701(3)	1	3.9(9)
Li1		0	0	0.064(5)	0.61(4)	2.8(1)
Mg1		0	0	0.064(5)	0.39(4)	2.8(1)
Mg2		0	0	0.341(4)	0.61(4)	2.8(1)
Li2		0	0	0.341(4)	0.39(4)	2.8(1)
B1		0.773(2)	0.537(1)	0.445(2)	1	0.2(3)
H11		0.85(1)	0.62(9)	0.48(6)	1	B_{B1}
H12		0.75(1)	0.56(7)	0.36(3)	1	B_{B1}
H13		0.65(5)	0.54(2)	0.49(6)	1	B_{B1}
H14		0.83(2)	0.43(7)	0.46(6)	1	B_{B1}
B2		0.560(6)	0.833(6)	0.70(4)	1	B_{B1}
H21		0.53(7)	0.80(1)	0.77(6)	1	B_{B1}
H22		0.52(6)	0.81(1)	0.62(7)	1	B_{B1}
H23		0.72(1)	0.77(2)	0.70(2)	1	B_{B1}
H24		0.63(3)	0.95(5)	0.70(1)	1	B_{B1}

Table S7 Selected interatomic distances in RbLiMg(BH₄)₄, for the structure refined at room temperature.

Rb-Rb	6.28(1)-7.88(2) Å
LiMg1-LiMg1	6.28(1)-7.88(2) Å
LiMg2-LiMg2	6.28(1)-7.88(2) Å
Rb-B	3.27(4)-3.94(3) Å
LiMg1-B	2.42(4)-2.44(2) Å
LiMg2-B	2.55(2)-2.62(2) Å
B-H	1.13(5) Å

Table S8 Atomic coordinates of RbLiMn(BH₄)₄, space group *Aba2*, $a = 8.266(1)$, $b = 9.477(2)$, $c = 12.616(2)$ Å, $V = 988(1)$ Å³, $Z = 4$ at *RT* as refined from synchrotron powder diffraction data measured at Diamond. Standard deviations for hydrogen atoms positions were retrieved by the boot strapping method implemented in TOPAS.

Atom	Site	<i>x</i>	<i>y</i>	<i>z</i>	Occupancy	B_{iso} [Å ²]
Rb1		0	0	0.701(3)	1	3.7(1)
Li1		0	0	0.0582(7)	0.23(7)	2.8(2)
Mn1		0	0	0.0582(7)	0.77(7)	2.8(2)
Mn2		0	0	0.336(2)	0.23(7)	2.8(2)
Li2		0	0	0.336(2)	0.77(7)	2.8(2)
B1		0.738(2)	0.513(2)	0.457(2)	1	2.0(3)
H11		0.78(6)	0.59(2)	0.52(7)	1	B_{B1}
H12		0.73(5)	0.57(1)	0.38(6)	1	B_{B1}
H13		0.62(4)	0.47(5)	0.48(8)	1	B_{B1}
H14		0.83(7)	0.42(5)	0.45(1)	1	B_{B1}
B2		0.590(1)	0.829(1)	0.696(2)	1	B_{B1}
H21		0.52(1)	0.80(2)	0.77(6)	1	B_{B1}
H22		0.52(1)	0.80(2)	0.62(6)	1	B_{B1}
H23		0.71(2)	0.77(3)	0.70(2)	1	B_{B1}
H24		0.62(4)	0.95(8)	0.70(6)	1	B_{B1}

Table S9 Selected interatomic distances in RbLiMn(BH₄)₄, for the structure refined at room temperature.

Rb-Rb	6.29(3)-7.89(3) Å
LiMn1-LiMn1	6.29(3)-7.89(3) Å
LiMn2-LiMn2	6.29(3)-7.89(3) Å
Rb-B	3.21(2)-3.89(3) Å
LiMn1-B	2.49(3)-2.51(4) Å
LiMn2-B	2.49(5)-2.51(4) Å
B-H	1.13(9) Å

Table S10 Atomic coordinates of $K_3Li_2Mg_2(BH_4)_9$, space group $P2/c$, $a = 11.321(1)$, $b = 10.181(1)$, $c = 11.737(2)$ Å, $\beta = 121.2(1)^\circ$, $V = 1157(2)$ Å³, $Z = 2$ at RT as refined from synchrotron powder diffraction data measured at SLS. Standard deviations for hydrogen atoms positions were retrieved by the boot strapping method implemented in TOPAS.

Atom	Site	x	y	z	B_{iso} [Å ²]
K1		0.5	0.0	0.75	5.5(2)
K2		0	0.5	0	5.5(2)
K3		0	0	0	5.5(2)
Li1		0.214(3)	0.756(4)	0.799(4)	2.4(3)
Mg1		0.302(7)	0.714(7)	0.404(3)	2.4(3)
B1		0.234(4)	0.796(5)	0.550(4)	3.0(4)
H11		0.33(2)	0.74(3)	0.58(2)	B_{B1}
H12		0.22(2)	0.80(2)	0.64(1)	B_{B1}
H13		0.14(2)	0.74(3)	0.47(2)	B_{B1}
H14		0.24(4)	0.89(9)	0.52(3)	B_{B1}
B2		0.210(4)	0.223(5)	0.660(4)	B_{B1}
H21		0.16(3)	0.19(3)	0.71(2)	B_{B1}
H22		0.21(4)	0.14(1)	0.59(3)	B_{B1}
H23		0.32(2)	0.25(6)	0.74(2)	B_{B1}
H24		0.15(5)	0.31(3)	0.59(3)	B_{B1}
B3		0.773(2)	0.490(2)	0.118(3)	B_{B1}
H31		0.85(9)	0.57(1)	0.18(2)	B_{B1}
H32		0.82(1)	0.39(7)	0.14(2)	B_{B1}
H33		0.73(1)	0.52(2)	0.01(7)	B_{B1}
H34		0.69(1)	0.49(2)	0.14(1)	B_{B1}
B4		0.534(2)	0.806(1)	0.520(6)	B_{B1}
H41		0.51(2)	0.701(7)	0.48(2)	B_{B1}
H42		0.58(2)	0.86(2)	0.47(2)	B_{B1}
H43		0.61(2)	0.81(2)	0.63(7)	B_{B1}
H44		0.44(2)	0.86(2)	0.49(2)	B_{B1}
B5		0	0.143(3)	0.25	B_{B1}
H51		-0.03(2)	0.207(3)	0.16(6)	B_{B1}
H52		0.09(6)	0.079(3)	0.28(2)	B_{B1}

Table S11 Selected interatomic distances in $K_3Li_2Mg_2(BH_4)_9$, for the structure refined at room temperature.

K-K	4.85(3)-7.78(3) Å
Li-Li	4.36(3)-7.89(2) Å
Mg-Mg	5.81(3)-7.32(4) Å
Li-Mg	4.76(3)-7.40(2) Å
K1-B	3.40(3)-3.67(2) Å
K2-B	3.50(3)-3.87(1) Å
K3-B	3.12(2)-3.28(1) Å
Li-B	2.41(5)-3.09(2) Å
Mg-B	2.35(3)-2.57(3) Å
B-H	1.12(7)-1.13(6) Å

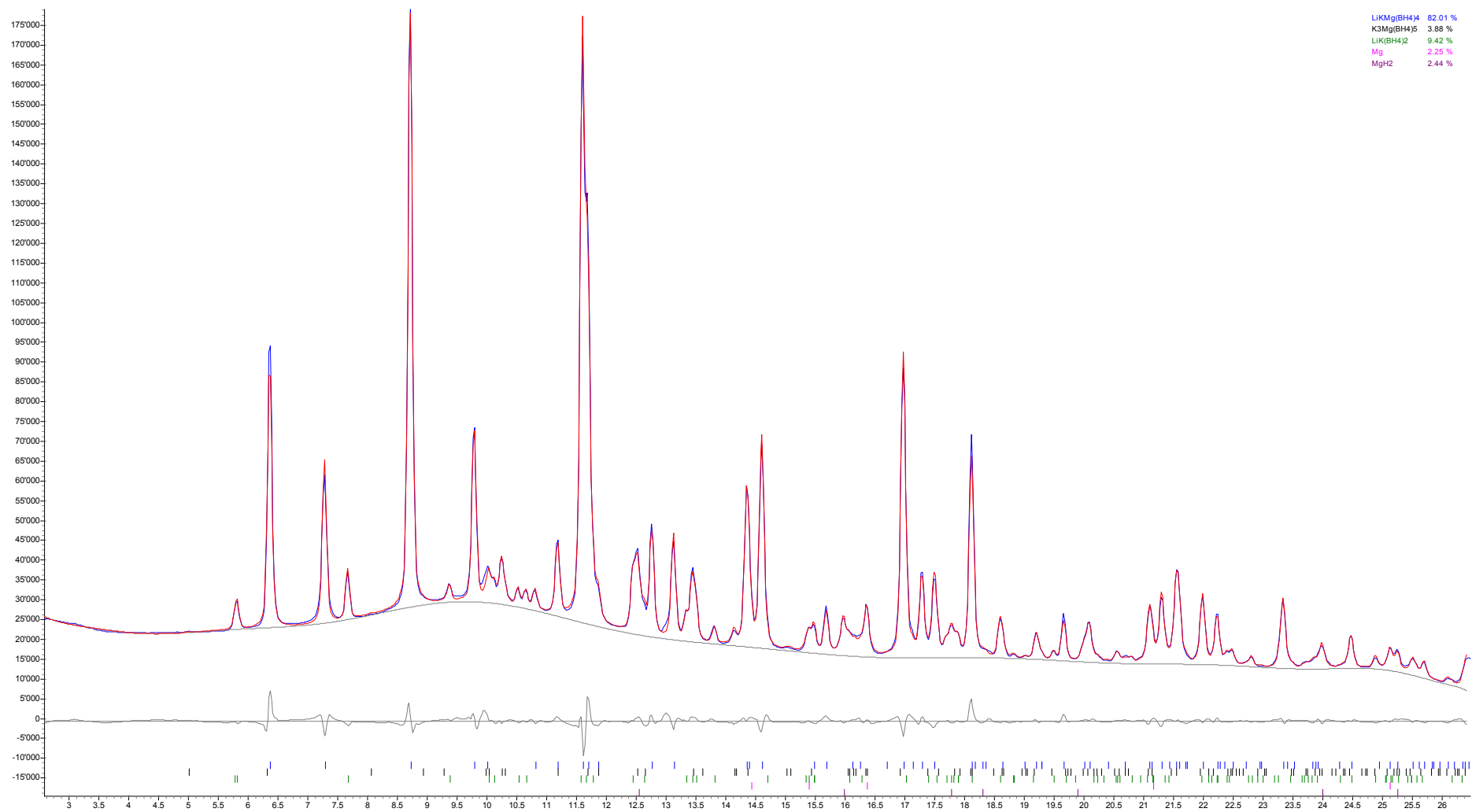


Figure S7. Rietveld plot generated by TOPAS for the sample measured at RT at SNBL; $\lambda = 0.69736 \text{ \AA}$. HKL ticks, from top to bottom: $\text{LiKMg}(\text{BH}_4)_4$, $\text{K}_3\text{Mg}(\text{BH}_4)_5$, $\text{LiK}(\text{BH}_4)_2$, Mg, MgH_2 . $R_{wp}(\text{bgr. corr.}) = 2.2\%$, $\chi^2 = 80$.

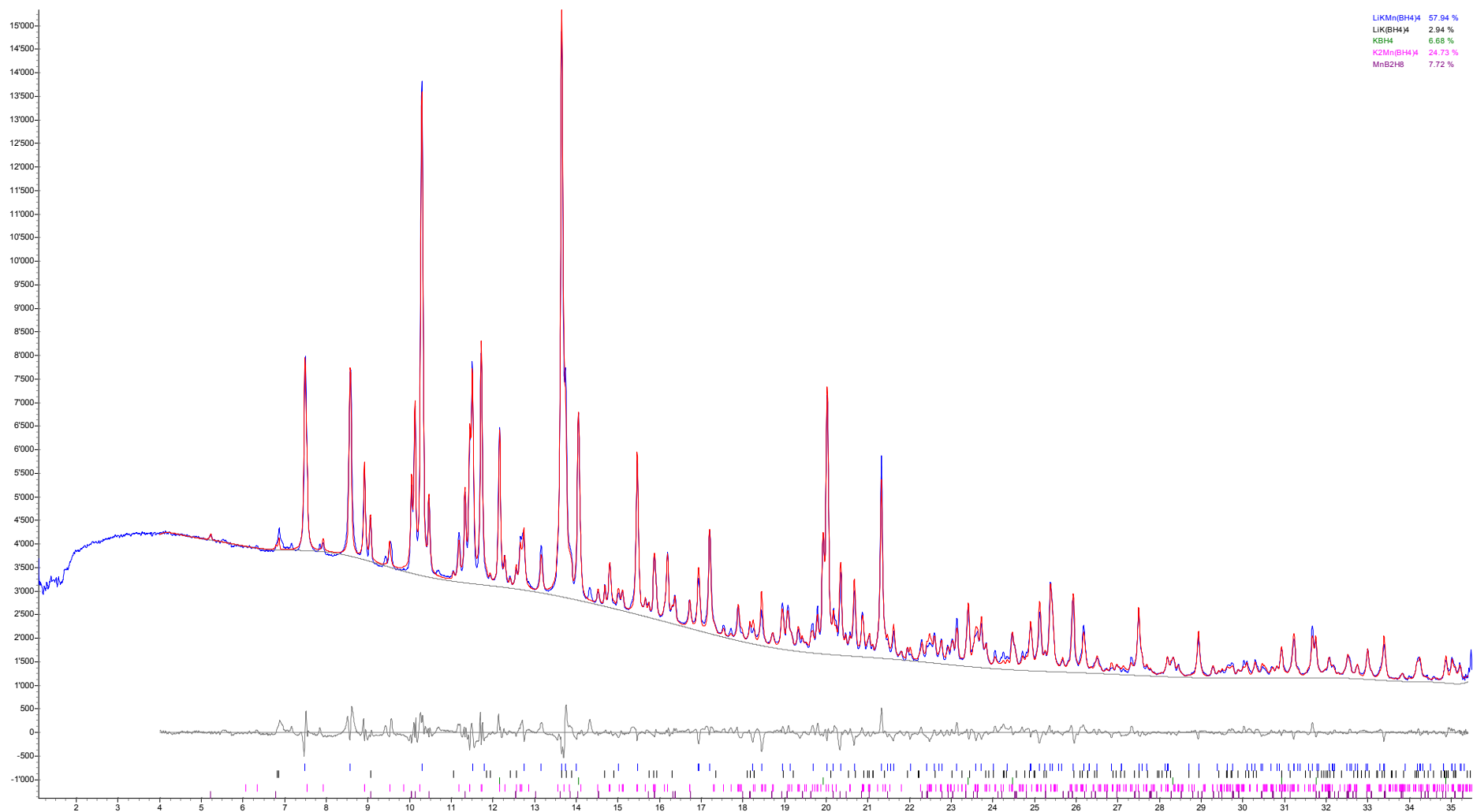


Figure S8. Rietveld plot generated by TOPAS for the sample measured at *RT* at SNBL; $\lambda = 0.82711 \text{ \AA}$. HKL ticks, from top to bottom: $\text{KLiMn(BH}_4)_4$, $\text{LiK(BH}_4)_2$, KBH_4 , $\text{K}_2\text{Mn(BH}_4)_4$, $\text{Mn(BH}_4)_2$. $R_{wp}(\text{bgr. corr.}) = 2.76\%$, $\chi^2 = 10.0$.

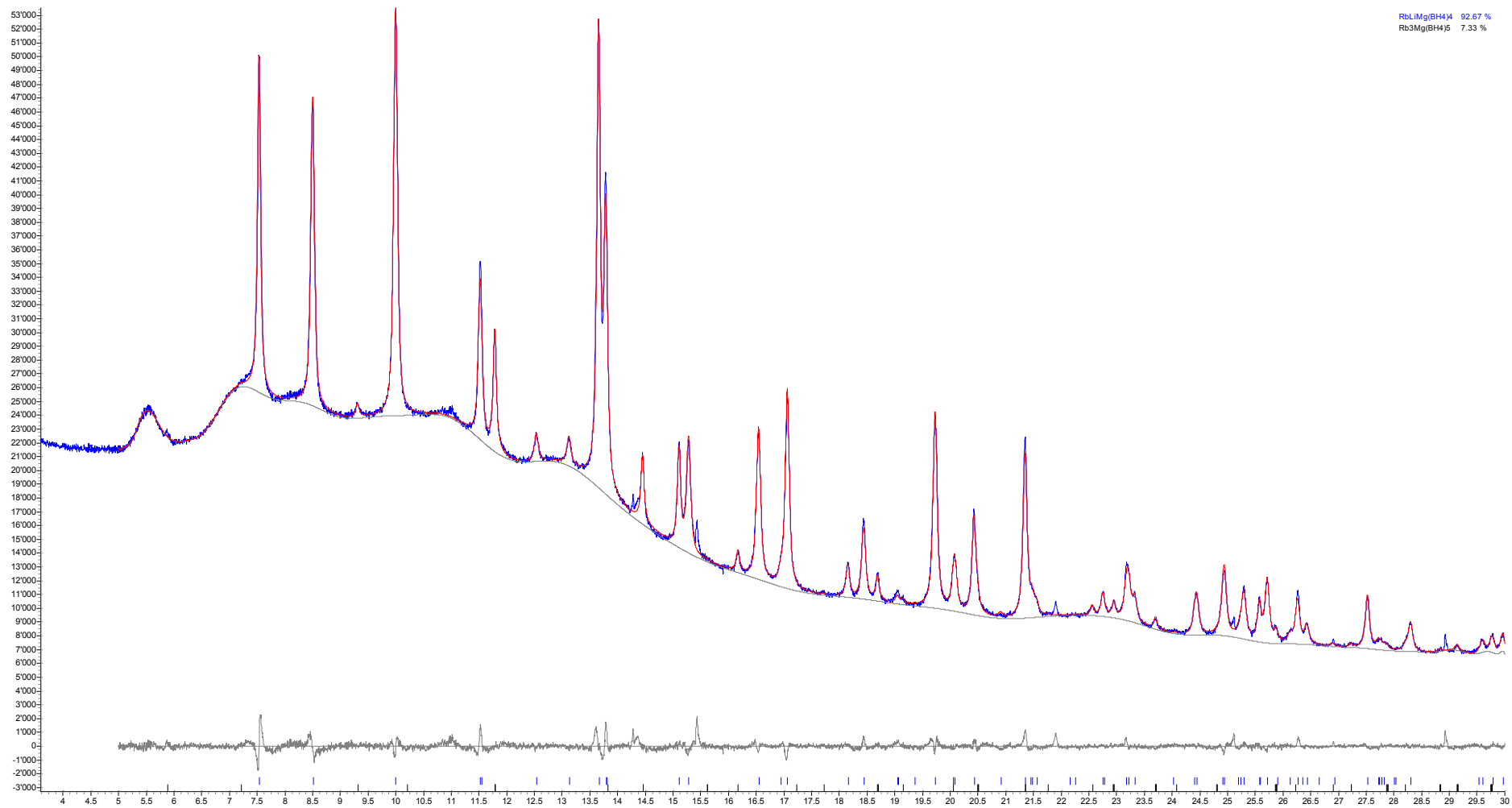


Figure S9. Rietveld plot generated by TOPAS for the sample measured at *RT* at SLS; $\lambda = 0.82711 \text{ \AA}$. HKL ticks, from top to bottom: $\text{RbLiMg}(\text{BH}_4)_4$, $\text{Rb}_3\text{Mg}(\text{BH}_4)_5$. $R_{wp}(\text{bgr. corr.}) = 1.26\%$, $\chi^2 = 1.55$.

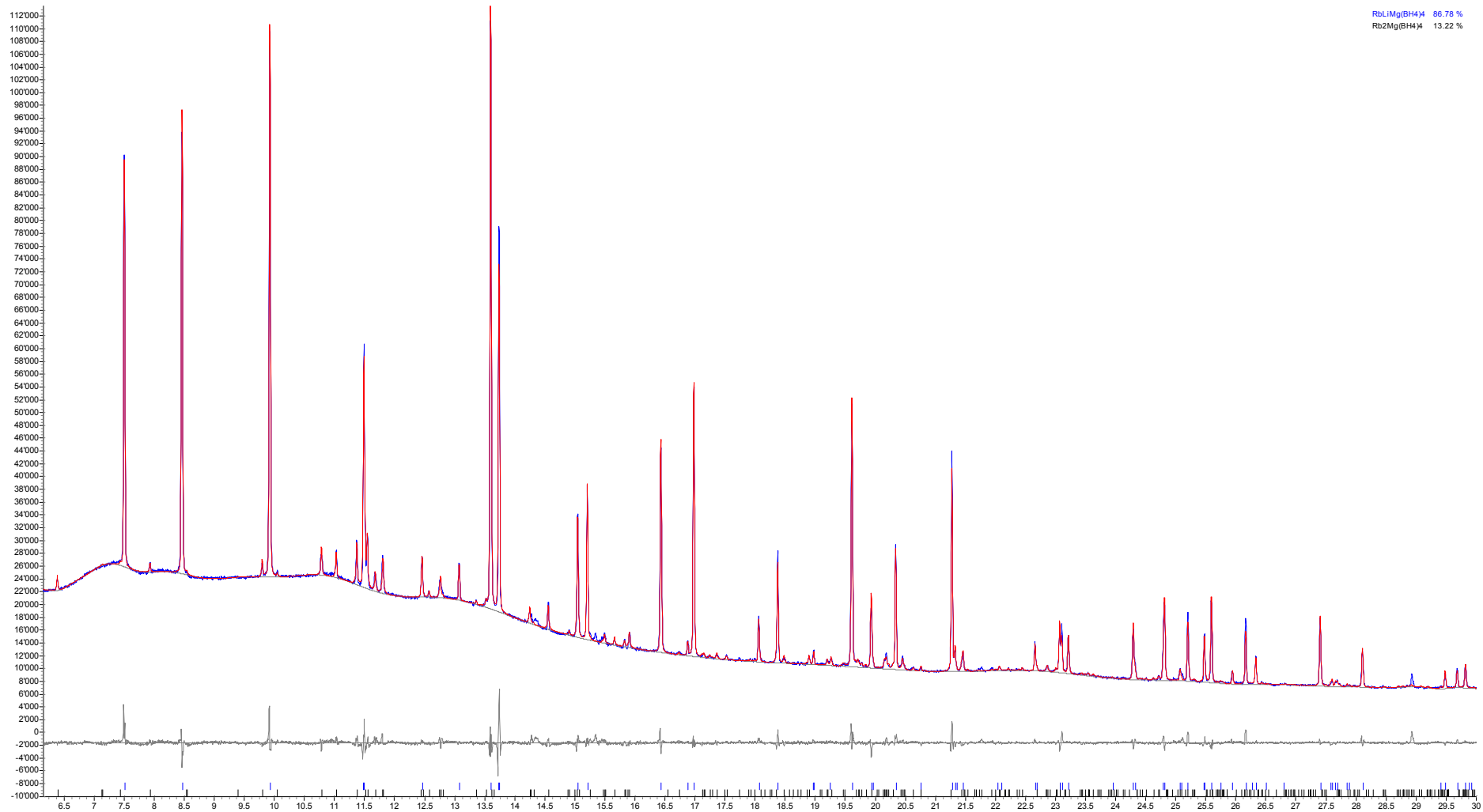


Figure S10. Rietveld plot generated by TOPAS for the sample measured at 373 K at SLS; $\lambda = 0.82711 \text{ \AA}$. HKL ticks, from top to bottom: RbLiMg(BH₄)₄, Rb₃Mg(BH₄)₅.
 $R_{wp}(\text{bgr. corr.}) = 1.33\%$, $\chi^2 = 1.59$.

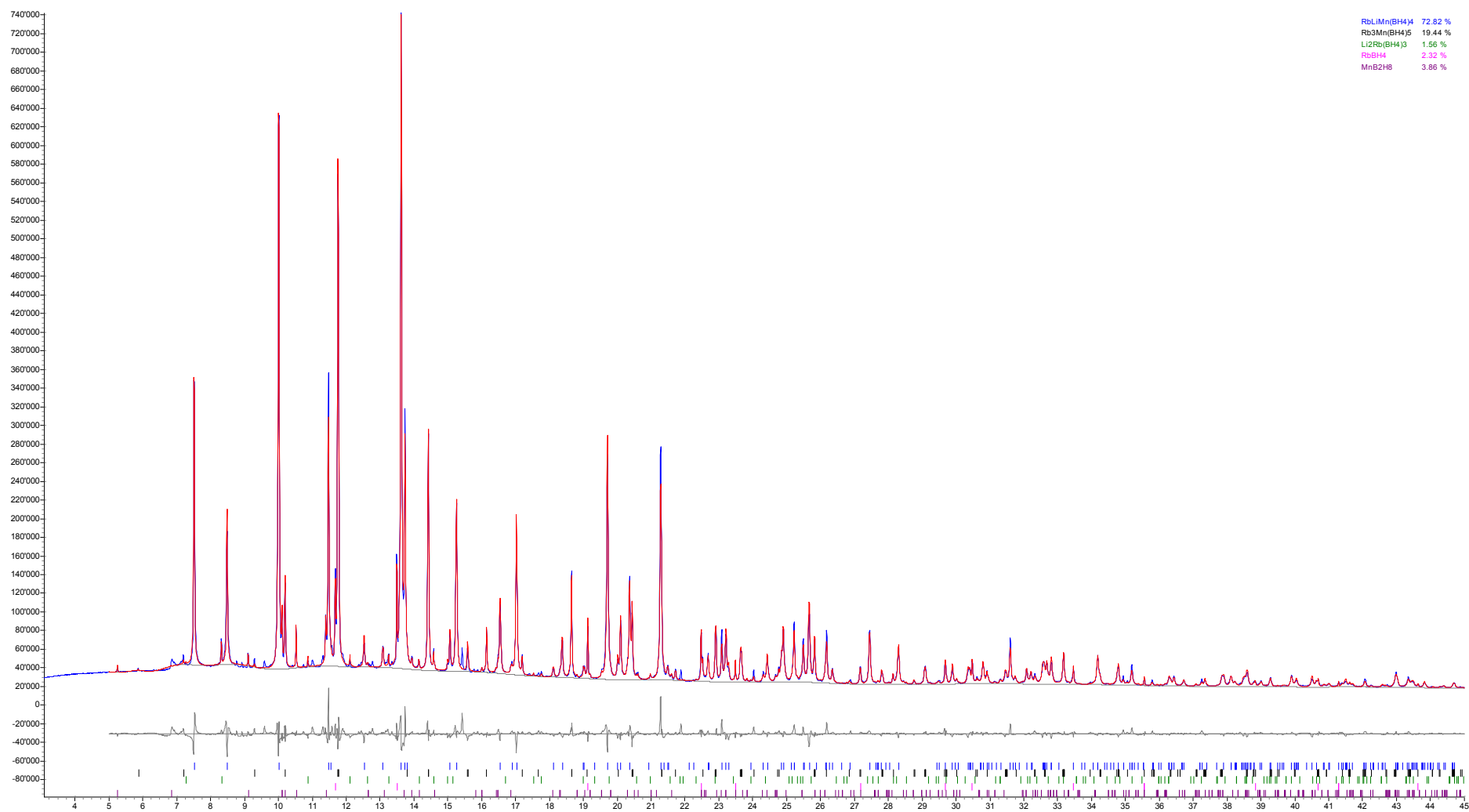


Figure S11. Rietveld plot generated by TOPAS for the sample measured at *RT* at Diamond; $\lambda = 0.82712 \text{ \AA}$. HKL ticks, from top to bottom: RbLiMn(BH₄)₄, Rb₃Mn(BH₄)₅, Li₂Rb(BH₄)₃, RbBH₄, Mn(BH₄)₂. $R_{wp}(\text{bgr. corr.}) = 4.58\%$, $\chi^2 = 9.2$.

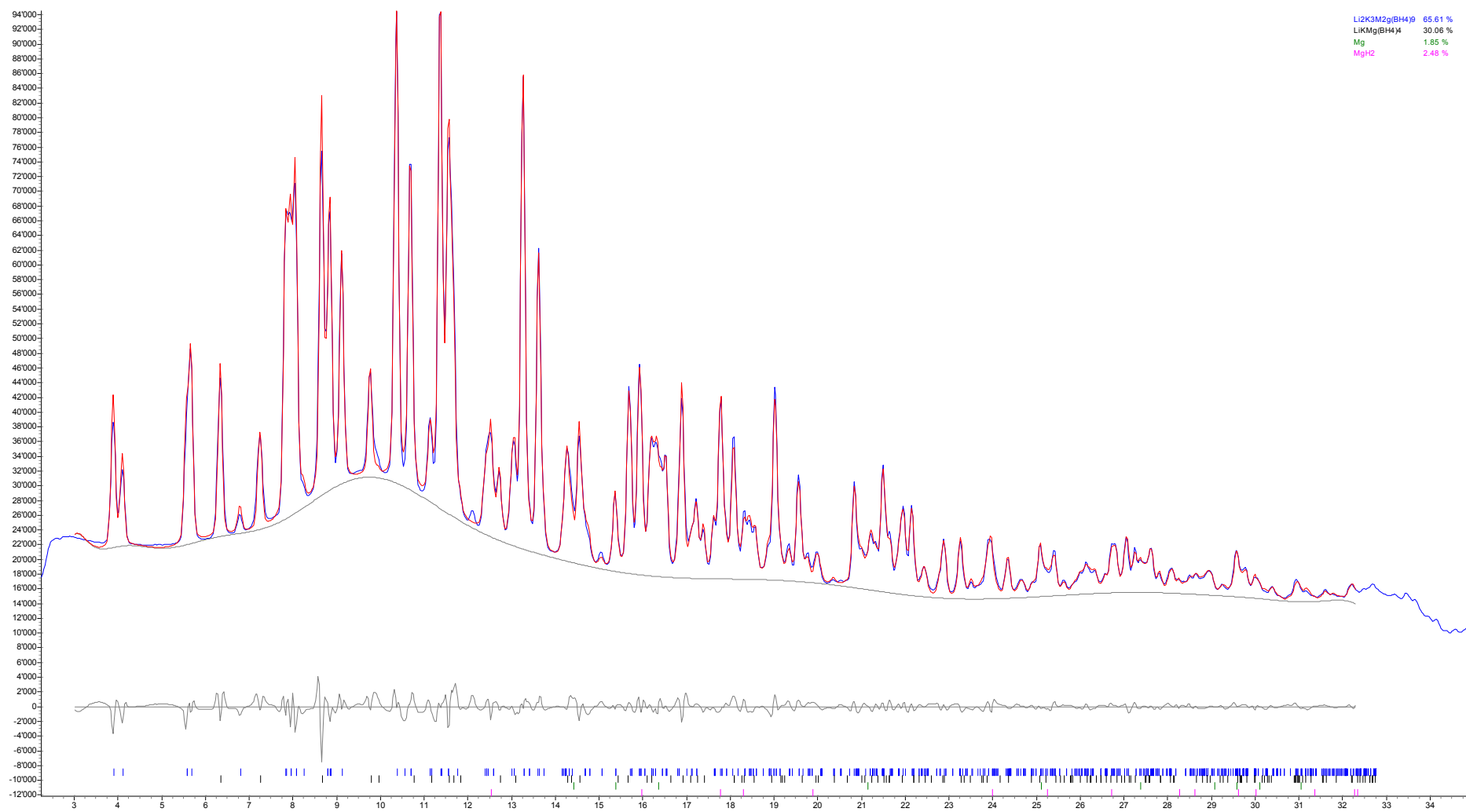


Figure S12. Rietveld plot generated by TOPAS for the sample measured at 350 K at SNBL; $\lambda = 0.69736 \text{ \AA}$. HKL ticks, from top to bottom: $\text{K}_3\text{Li}_2\text{Mg}_2(\text{BH}_4)_9$, $\text{LiKMg}(\text{BH}_4)_4$, Mg, MgH_2 . $R_{wp}(\text{bgr. corr.}) = 2.04\%$, $\chi^2 = 73$.

